Electron diffraction for analysing crystal orientation of thin films

Holm Kirmse, Johannes Müller und Christoph T. Koch

AG Strukturforschung / Elektronenmikroskopie

1. The goal

In this practicum you are expected to:

- understand the experimental setup of an electron diffraction camera,

- understand the relationship between camera length, lattice vectors, Miller indices, wavelength, and distances in diffraction patterns,

- record diffraction patterns on digital cameras with both light and 200 keV electrons,

- index electron diffraction patterns

This goal will be achieved by splitting up the 1-day practicum into two parts:

1. Diffraction of light by a two-dimensional grating on an optical bench

2. Diffraction of relativistic electrons by the three-dimensional lattice of a crystal.

2. Introduction: Diffraction, crystals, electron waves, and the transmission electron microscope

In this section some of the fundamental physical concepts relevant to this practicum will be recalled.

2.1. Diffraction of light by an optical grating

If monochromatic and spatially coherent (laser) light transmits a transparent diffraction grating with perpendicular diffraction slits being separated by the distance d along the

horizontal x-axis a diffraction pattern with discrete diffraction orders is formed. Constructive interference of light emitted by each of the slits in the diffraction grating shown in Fig. 1 leads to horizontally separated diffraction spots at angles θ_m for which holds

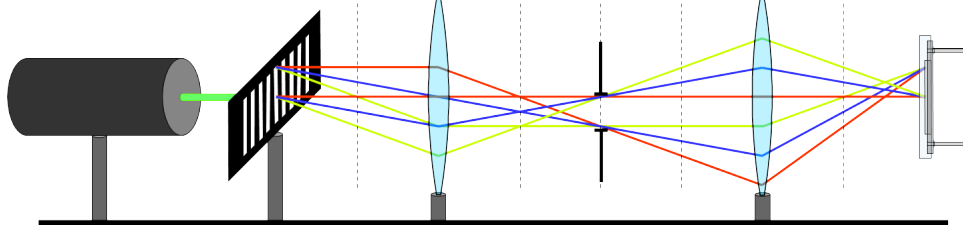$$\sin(\theta_m) d = m\lambda \tag{1}$$

Figure 1: Experimental setup of diffraction of laser light by an optical grating and its projection onto a detector by an optical setup consisting of an objective lens, and objective aperture, and a projector lens.

For the more complex discussion of electron diffraction from a three-dimensional lattice it is useful to describe this phenomenon in momentum space. Let's define the direction of the incident laser light as the direction of the optical axis of the system. The momentum vector of the incident radiation is then given by

$$\vec{k}_0 = (k_x, k_y, k_z) = \left(0, 0, \frac{2\pi}{\lambda}\right) \tag{2}$$

the diffracted radiation behind the diffraction grating is now split up into partial waves with momenta

$$\vec{k}_l = \left(\frac{2\pi \sin\theta_m}{\lambda}, 0, \frac{2\pi \cos\theta_m}{\lambda}\right) = \left(\frac{2\pi m}{d}, 0, \frac{2\pi \cos\theta_m}{\lambda}\right) \tag{3}$$

The discrete k_x-components of the scattered wave vectors may are obviously independent of the wavelength and only a function of the scattering object. They are thus called reciprocal lattice points along the horizontal momentum axis at distances

$$g_m = \frac{2\pi m}{d} \tag{4}$$

away from the momentum vector of the unscattered partial wave which is equal to that of the incident light $\vec{k}_0$.

A three-dimensional lattice may have separate periodicities along three different non-colinear directions $\vec{a}$, $\vec{b}$, and $\vec{c}$. The reciprocal lattice vectors are then indexed not by a single index m, but by the three (Miller) indices h, k, and l. The corresponding lattice vector is thus given by

$$\vec{g}_{h,k,l} = \left(h\vec{a}^*, k\vec{b}^*, l\vec{c}^*\right) \tag{5}$$

2

$$\vec{a}^* = 2\pi \frac{\vec{b} \times \vec{c}}{V_{cell}} \tag{6}$$

$$\vec{b}^* = 2\pi \frac{\vec{c} \times \vec{a}}{V_{cell}} \tag{7}$$

$$\vec{c}^* = 2\pi \frac{\vec{a} \times \vec{b}}{V_{cell}} \tag{8}$$

$$V_{cell} = \vec{a} \cdot \left(\vec{b} \times \vec{c} \right) \tag{9}$$

If we now place a recording screen at some camera length L away from the diffraction grating we expect the spots on the screen to appear at distances

$$x_m = L \tan\left(\theta_m\right) = L \tan\left(\text{asin}\left[\frac{m\lambda}{d}\right]\right) \approx L\lambda g_m \tag{10}$$

and

$$\vec{x}_{h,k,l} \approx L\lambda \vec{g}_{h,k,l} \tag{11}$$

The factor $L\lambda$ is also called the *calibration factor*.

2.2. Electron waves

Louis de Broglie in his 1924 doctoral thesis [6] proposed the wave nature of mass-carrying particles, giving them the wavelength

$$
\begin{aligned}
\lambda &= \frac{h}{p} = \frac{h}{\sqrt{\frac{E_{total}^2 - m_0^2 c^4}{c^2}}} \\
&= \frac{hc}{\sqrt{(E_{kin} + m_0 c^2)^2 - m_0^2 c^4}} = \frac{hc}{\sqrt{eV_0(2m_0 c^2 + eV_0)}}
\end{aligned}
\tag{12}
$$

(h being Planck's constant, m_0 the electron rest mass, and $E_{kin} = |eV_0|$ the kinetic energy of the electron, with e being its charge and V_0 the accelerating voltage) is very short, almost 2 orders of magnitude shorter than typical X-ray wavelengths. For electron beam energies achievable in a standard TEM, i.e. $E \geq 20$ kV, the wavelength can be approximated by the following expression:

$$\lambda \approx -0.0040\text{Å} + \frac{0.408\text{Å}}{\sqrt{E/\text{keV}}} \tag{13}$$

For example, in a standard medium voltage TEM ($U = 200$ kV) the electron wavelength is $\lambda = 0.0251$ Å.

Only 3 years after the revolutionary discovery of the wave nature of electrons, electron diffraction, a phenomenon based on the wave nature of these small particles, was able to provide diffraction patterns of crystalline materials very similar to those obtained by X-rays [4, 5, 18]. Today, electron diffraction has developed into a very powerful tool in

structural crystallography and materials science and has again split into several sub-disciplines. In light of the large body of literature available on electron scattering and diffraction it seems important to emphasize that within this chapter the term 'diffraction' is treated synonymously with 'elastic scattering', i.e. a process which preserves the energy of the incident electron.

If the accelerating voltage of the electron is in the range of 20 - 200 V (sometimes up to 600 V) one speaks of low-energy electron diffraction (LEED). Electrons of this energy have a wavelength of about 1 Å(2.7 Å at 20 V and 0.5 Å at 600 V), i.e. comparable to the distance between atoms, and can only penetrate the first atomic layers, or 5-10 Å of the sample. LEED is therefore exclusively used to study the atomic structure of surfaces, mainly under ultra-high vacuum conditions. At higher beam energies, as in medium energy electron diffraction (MEED, accelerating voltage between 1 kV and 5 kV [14]) or reflection high energy electron diffraction (RHEED, electron energy range between 40 keV and 100 keV) the scattering angles become too small to work with a normally incident electron beam, but instead, a more (RHEED) or less (MEED) grazing incidence setup has to be chosen. This deviation of the angle of incidence from the surface normal makes RHEED much more sensitive to surface roughness than LEED, with MEED being about in between both worlds [2].

At sufficiently high energy (above 20 keV) electrons are fast enough to penetrate several nanometers of material without too much absorption or charging. Although transmission through very thin samples and even atomic resolution imaging is also possible at lower energy [9], transmission electron diffraction in transmission electron microscopes (TEMs) is most commonly done at accelerating voltages above 20 kV and in some cases up to 1 or even 3 MV. Because of the versatility of TEMs and their availability in a large number of laboratories around the globe this chapter will focus on transmission high energy electron diffraction (HEED) only.

Electron Diffraction patterns of crystalline materials contain a wealth of information and have helped to reconstruct the atomic positions of complex crystal structures [7, 19, 20], largely by applying the very same techniques developed in X-ray crystallography. However, being limited in space, the final section of this chapter will only be able to provide an overview of a selection of electron diffraction techniques which showcase the unique capabilities of electron diffraction compared to other (e.g. X-ray or neutron) diffraction techniques.

The electric charge of the electrons not only allows them to be accelerated by electrostatic fields, but also deflected and focused by both, magnetic as well as electric fields according to the Lorentz force

$$\vec{F}_{\text{Lorentz}} = -e\left(\vec{E} + \vec{v} \times \vec{B}\right) \tag{14}$$

While round magnetic lenses have an inherent positive spherical aberration [16], multipole elements may be used to compensate this spherical (and also higher order) aberrations [10, 13], producing electron probes as small as 0.5 Å in diameter [11].

In addition to the correction of lens aberrations in the probe-forming lens system the formation of such small probes also requires a high spatial coherence. A critical parameter

describing the amount of current available at a certain degree of spatial coherence is the brightness β, which is the amount of current emitted into a certain solid angle Ω from an area A. For rotationally symmetric systems one can also write

$$\beta = \frac{I}{\Omega A} = \frac{I}{(\pi \alpha r)^2} \tag{15}$$

where α is the angular radius of the cone of emitted electrons, and r the radius of the source. Because of the increased momentum of electrons at higher accelerating voltages, the effective cone radius α is proportional to the electron wavelength, and, from equation (12) is thus inverse proportional to the square root of the electron's kinetic energy. For this reason the reduced brightness

$$\beta_r = \beta / U \tag{16}$$

is often used instead. The electron microscope used for this practicum has a field emission gun (FEG) [3]. A FEG, today the standard electron source in high-performance TEMs, provides a source of nanometer dimensions and sub-eV energy spread, with a brightness per unit bandwidth greater than current-generation synchrotrons [17]. When also taking into account the much stronger interaction of electrons with matter, the amount of coherently scattered signal that can potentially be collected from a certain volume of material exceeds even that of free-electron lasers. FEGs have a much higher brightness than thermionic electron guns, such as a LaB_6 source used, for example in the Hitachi 8100 or the JEOL JEM2100 (both operating within the HU physics building).

2.3. Diffraction of electron waves by a three-dimensional lattice

Due to fact that the electrons in an atom are much more delocalized than its protons, every (neutral) atom produces a sharply peaked positive electrostatic potential with the center of this peak at the position of the core of this atom. According to equation (14) electrons are deflected by electrostatic and magnetic fields. Neglecting any magnetic contributions to the scattering the electrons are thus deflected by the electrostatic potential of atoms. Since in crystalline specimen the atoms are located on a regular lattice in three-dimensional space we can describe the scattering property of the whole crystal by only describing the electrostatic potential of its unit cell in reciprocal space. The Fourier coefficients of the electrostatic potential of the unit cell are called structure factors and are given by

$$U(\vec{g}) = \frac{\gamma}{V_{cell}} \sum_j f_{el}^j \left(\frac{|\vec{g}|}{2} \right) \exp\left(2\pi i \vec{r}_j \cdot \vec{g} \right) \tag{17}$$

where $\gamma = 1/\sqrt{1 - v^2/c^2}$ is the Lorentz factor for the fast electron at velocity v, V_{cell} is the unit cell volume, $f_{el}^j(s)$ is the atomic scattering factor for scattering parameter $s = |\vec{g}|/2$, $\vec{g}$ is a reciprocal lattice vector, and $\vec{r}_j$ is the position of the jth atom within the unit cell. The atomic scattering factor is the radial part of Fourier transform of the electrostatic potential of the atom j alone. Since the potential of an isolated atom is

isotropic in angle and not infinitely sharply peaked, this scattering factor falls of with scattering parameter s. It can be well approximated by the sum of a 4 Gaussians [8].

The electron structure factors are only non-zero on points in reciprocal space which lie on the reciprocal lattice. However, this reciprocal lattice is convoluted by the shape transform of the crystal, i.e. the Fourier transform of its shape in real space. Since TEM specimen must be very thin for the electron beam to be able to pass through them, but may be very wide laterally, the reciprocal lattice points have some finite extent along the direction parallel to the wave vector of the incident electron beam, but are very sharply defined in the lateral directions. For nanocrystals, which are also laterally confined, the reciprocal lattice points extend also laterally. As illustrated in Figure 2 elastically scattered electrons maintain their momentum and may therefore scatter only to reciprocal lattice vectors which lie on a sphere (Ewald sphere). Reflections which are not intersected by the Ewald sphere may still be excited, but, because of the non-vanishing excitation error s_g (reciprocal space distance between the Ewald sphere and the reciprocal lattice point for the infinitely extended crystal), in most cases with a reduced intensity.

Kinematical scattering theory, which neglects the possibility that an electron scatters more than once on its path through the sample predicts that the intensity in the diffraction pattern $I_{h,k,l} \propto |U(\vec{q})|^2$, i.e. that it is proportional to the amplitude squared of the structure factor $U(\vec{g}_{h,k,l})$.

For elastic scattering of the incident electron wave the kinetic energy of the electron is preserved, and with that also the absolute value of its momentum vector. This means that in reciprocal space the wave vectors of all scattered electrons must lie on the surface of a sphere of the Figure 2 illustrates

2.4. Optical systems built of lenses

For setting up the optical diffraction camera, and for understanding the electron diffraction experiment it is important that you review the following principles of geometrical optics:

- The lens equation $d_{object}^{-1} + d_{image}^{-1} = f^{-1}$.

- The magnification of an image: $M = h_{image}/h_{object} = d_{image}/d_{object}$.

- The fact that in the back focal plane a lens produces the Fourier transform of the light field in the object plane.

2.5. Experimental setups of an optical diffraction camera and an electron microscope

2.5.1. The transmission electron microscope (TEM)

Based on the Lorentz force given by equation (14) it has been discovered by Busch [1] that magnetic coils will focus an electron beam. This has soon after led to the development of
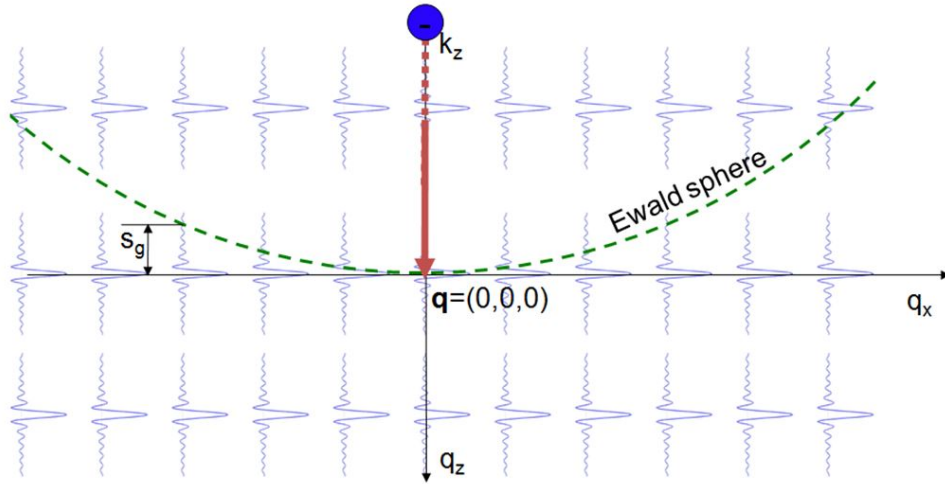
Figure 2: Diagram illustrating the Ewald sphere construction and the physical meaning of the excitation error s_g. The fast beam electron can only scatter elastically to reciprocal space vectors which lie on the Ewald sphere (dashed curve). The distance between a given point in reciprocal space and the Ewald sphere in the direction of the specimen's surface normal (assumed to be in the z-direction in this illustration) is called excitation error s_g.

the first transmission electron microscope (TEM) by Knoll and Ruska [12] an achievement which has been honoured with the Nobel price in 1986 [15]. Modern TEMs are equipped with at least 4 electromagnetic lenses (gun lens and condenser lens system and objective pre-field lens) to collimate or focus the beam on the sample and at least 4 lenses below the sample (objective lens and a projector lens system) to focus either a magnified image or the magnified diffraction pattern on a detector which can be a CCD camera, photographic film, digital imaging plates, or a spectrometer. In this practicum we will use a CCD camera for detecting images and diffraction patterns.

Figure 3 shows that by simply changing the current running through lenses in the projector lens system the TEM can switch between image and diffraction mode. Likewise, the condenser lens system can be used to continuously vary the illumination convergence angle and with that the size of the electron probe on the sample, changing from parallel to convergent illumination, facilitating parallel or convergent beam electron diffraction (CBED).

The area of the sample contributing to the diffraction pattern in parallel-beam illumination (Figure 3b) may be selected in 2 ways: a) by an aperture in the condenser lens system or b) by a selected area aperture in the position of the first intermediate image (indicated by an arrow in Figure 3b). In this practicum we will use selected area electron diffraction (SAED), i.e. apply the second option of selecting the contributing area. The reason for this is the experimental simplicity. Without changing any lens currents or alignment, or the illumination conditions on the sample we may quickly switch between a very large field of view for recording an overview image and a small field of view for

Imaging   **Diffraction**

Specimen

Objective lens

Back focal plane

Intermediate image plane

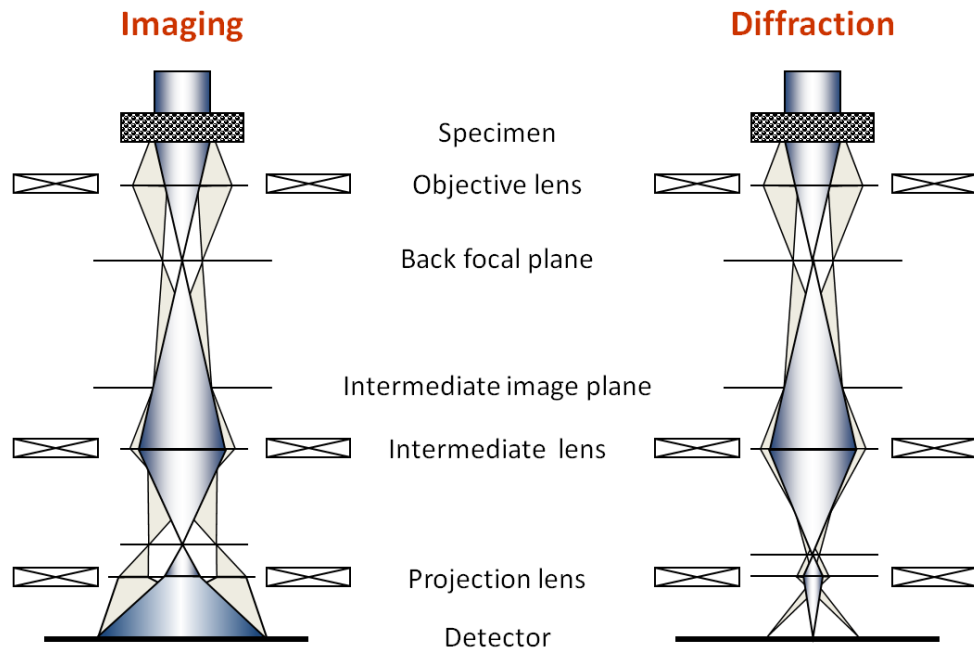Intermediate lens

Projection lens

Detector

Figure 3: Two different modes of operation of a TEM: a) High-resolution imaging mode: An incident plane wave scatters elastically according to the different lattice planes and the diffracted beams interfere with each other. This interference pattern may in some cases be interpreted as directly representing the atomic structure. b) For parallel illumination the diffraction mode is a (conventional) spot pattern.

selecting the area from which the diffraction data shall stem, simply by inserting and positioning a small aperture. There are a few problems of this approach: a) Because of the fixed magnification of the objective lens the smallest area that can be selected by a very small (e.g. 5 µm aperture) has typically a diameter not much smaller than 80 nm. b) Due to aberrations of the objective lens high-angle diffraction information may stem from a slightly larger area than the one selected from the (bright-field) image.

3. Experiment 1: Diffraction of light by a two-dimensional grating

The first half of this practicum consists in setting up an optical diffraction experiment in which the diffraction pattern produced by a laser shining on a test target with known diffraction gratings is to be properly imaged by a CCD camera. This experiment consists of the following steps:

1. Design an optical system with a magnification of 1 that illuminates the test target, has an aperture in an intermediate image plane to select areas with different spacings on the test target and a camera to image either the diffraction pattern or an image of the selected area on the test target. The test target is mounted on a sample holder and can be alligned perpendicular to the optical axis. This setup corresponds very closely to that of the transmission electron microscope, but is much more intuitively accessible. The parameters are:

   - Focal length of the optical lenses: $f = 150$ mm
   - Grating spacings: $s_1 = 33$ µm to $s_{13} = 6.6$ µm (periodicity: $p_1 = 30$ lines/mm to $p_{13} = 150$ lines/mm in steps of 10 lines/mm)
   - Maximum length of the optical system: 1.5 m
   - Camera chip: Size: 7.11 mm x 5.34 mm, Pixel size: 3.69 µm x 3.69 µm, number of pixels: 1928 x 1448
   - Laser: green, $\lambda = 532$ nm, with beam expander

2. Use the optical bench set-up in the optics laboratory of the AG-SEM to implement your design.

3. Record an image and the corresponding diffraction pattern of two different diffraction gratings on the test target.
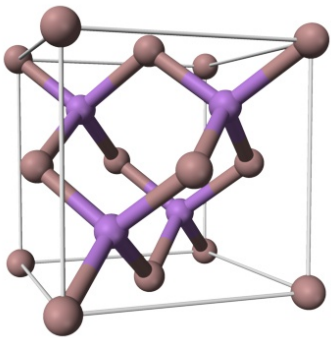
In your report the following details are expected:

- A detailed description of both of your designs for an appropriate imaging / diffraction camera satisfying above conditions.

- Include copies of the images you recorded using the CCD camera. You may invert the contrast of the diffraction pattern to make the diffraction spots more easily visible.

- Calculate the effective camera length L and the magnification M of your optical system.

- Discuss what happens when you reduce the spacing of the diffraction grid. Under what conditions are you able to record diffraction patterns of grids with a spacing of 0.5 nm, i.e. those of materials like Si or GaAs?

4. Experiment 2: Diffraction by the lattice of a crystal

Transmission electron diffraction
Lattice plane distances of different compound
semiconductors having sphalerite structure

Set of lattice planes	Compound semiconductor								
	GaP	GaAs	ZnSe	InP	InAs	CdSe	GaSb	ZnTe	CdTe
a (Å)	5.450	5.653	5.667	5.870	6.058	6.081	6.091	6.104	6.481
111	3.147	3.264	3.272	3.389	3.498	3.511	3.517	3.524	3.742
200	2.725	2.827	2.834	2.935	3.029	3.041	3.046	3.052	3.241
220	1.927	1.999	2.004	2.075	2.142	2.150	2.153	2.158	2.291
222	1.643	1.704	1.709	1.770	1.827	1.833	1.837	1.840	1.954
311	1.573	1.632	1.636	1.695	1.749	1.755	1.758	1.762	1.871
400	1.363	1.413	1.417	1.468	1.515	1.520	1.523	1.526	1.620
420	1.219	1.264	1.267	1.313	1.355	1.360	1.362	1.365	1.449
422	1.112	1.154	1.157	1.198	1.237	1.241	1.243	1.246	1.323
115 / 333	1.049	1.088	1.091	1.130	1.166	1.170	1.172	1.175	1.247

Figure 4: Left: Structure of GaAs. The lattice parameter of this cubic zinc blende structure, in which two atom types form two interpenetrating face-centered cubic lattices, is $a = 5.6535$Å. Right: Table of lattice parameters and lattice plane distances for different zinc blende structures.

The second half of this practicum will be carried out at the JEOL JEM2200FS FEG-TEM operated by the AG-SEM. The experiment consists of the following steps:

1. Record a diffraction pattern of the GaAs substrate of the specimen provided to you. Chose a camera length that allows at least three diffraction orders to be recorded on the CCD camera. Position the specimen relative to the SAA as shown in Fig 6 (bottom-left).

2. Using the same camera length, record a diffraction pattern of the layer on top of the GaAs substrate. Position the specimen relative to the SAA as shown in Fig 6 (bottom-right).
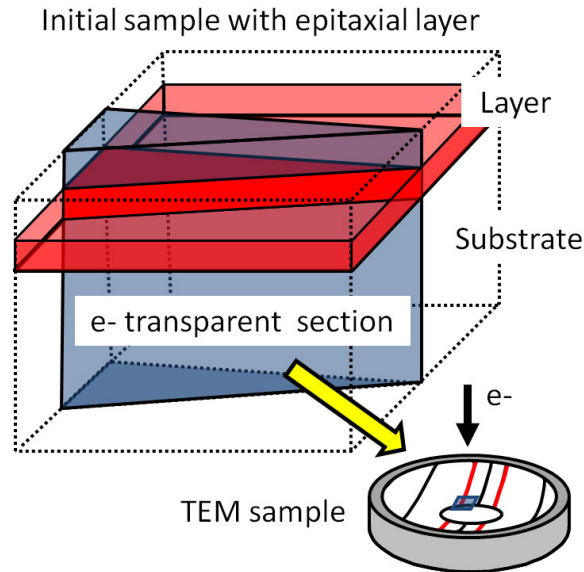
Figure 5: Diagram showing how the TEM lamella was prepared from the substrate and thin film: The sample to be used for this experiment was prepared in cross section. This means that the layer system is finally viewed edge-on. The preparation steps include mechanical thinning and final Ar+ ion milling. This carefully chosen strategy results in a wedge-shape of the area transmittable to the 200 keV electrons. Moreover, four regions are generated where the layer system can be observed. One of those areas is marked in blue.

3. Measure the distance of the four linearly independent reflections closest to the undiffracted beam relative to the position of the undiffracted beam.

In your report the following details are expected:

- Using the online software WebEMAPS (http://emaps.mrl.uiuc.edu/) Simulate (kinematic) diffraction patterns of GaAs in the following orientations [100], [110], and [111].

- Determine which indices h, k, and l the reflections you have measured might correspond to (the unit cell parameter of GaAs in the zinc blende structure is $a = 5.6535$Å) and determine the zone axis of the crystal you have investigated. Note: the zone axis must be perpendicular to all the reflections in the zero-order Laue zone, i.e. to the reciprocal lattice vectors appearing close to the undiffracted beam.

- Determine the calibration factor $L\lambda$ that is required to make your measurements agree best with the expected reciprocal lattice vectors.

- Identify the material of the thin film. Use the table provided in Fig. 4 to relate the lattice spacings you have measured with one of those materials.
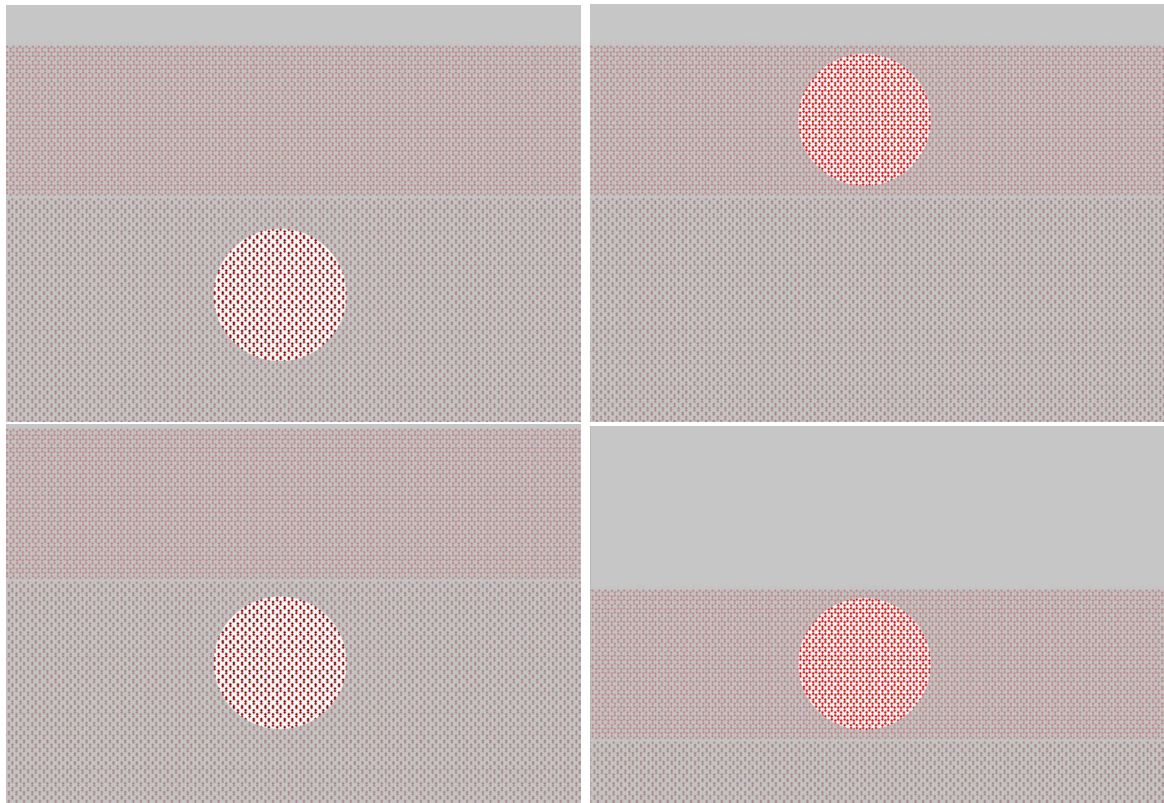
Figure 6: Illustration of how to position the specimen relative to the selected area aperture (SAA). Left: diffraction from substrate. Right: Diffraction from layer. In the top row the aperture is moved, and in the bottom row the sample is being moved. Please note: In order to minimize pattern distortions the SAA should remain in the same position, and only the sample should be moved.

- Discuss how the position of a diffraction spot varies with wavelength and unit cell parameter of the material

- Discuss how the accuracy of your measurement of the lattice parameter can be improved

- In which plane of the microscope setup is the diffraction pattern of the crystal generated, and which lens is used to focus this diffraction pattern on the camera?

- How does the illumination of the microscope need to be adjusted in order to produce sharp diffraction spots on the detector?

A. Step by step instruction for electron diffraction in the TEM

1. Find the position of the layer system

- Trackball: Move the specimen to find the appropriate position

- Push STD Focus

- Z-control (GP) + IMAGE WOBB (RP): Adjust the eucentric height

- Deactivate IMAGE WOBB
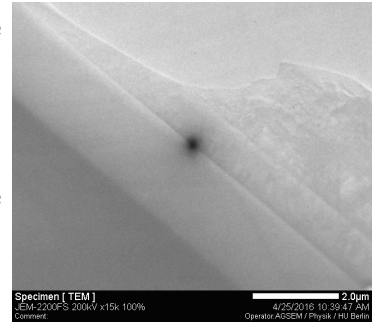
2. Zoom into the substrate area near the interface between GaAs substrate and layer 1

- Magnification (RP): Go to 50 kx

- BRIGHTNESS (LP): Adjust intensity

- FOCUS (RP): Adjust image sharpness
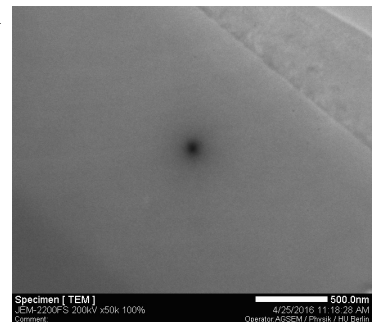
3. Insertion of the field-limiting aperture No 1

- Aperture control (LP): Select SAA + 1

- Center aperture using X and Y buttons
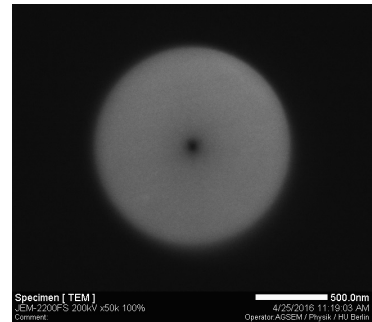
4. Switch to diffraction mode and converge the beam for high intensity

- Imaging/diffraction control (RP): Press SA DIFF

- Brightness (LP): Condense the beam by turning counter-clockwise (CCW)
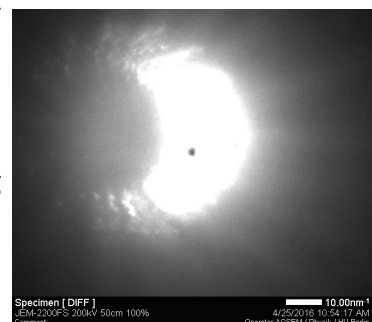
5. Insert high contrast aperture No 1

   - Aperture control (LP): Select HCA + 1
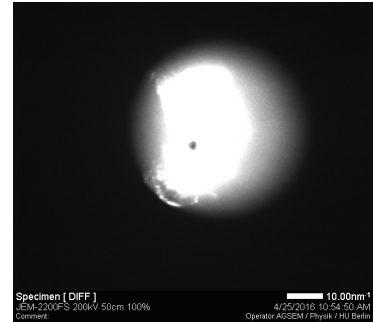
6. Focus on the back focal plane of the objective lens

   - Diffraction focus (RP): Focus the edge of the high-contrast aperture (HCA)

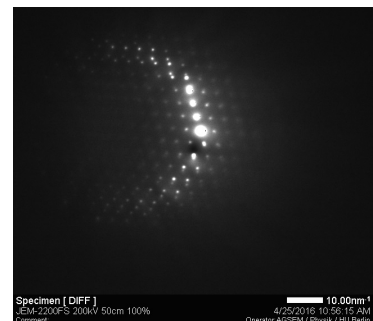   - **From now on, don't touch the diffraction focus!**
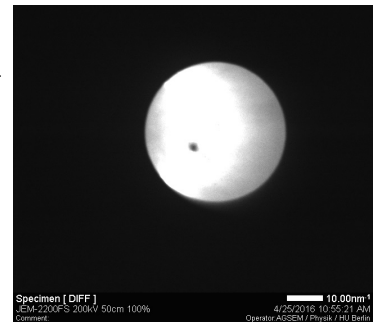
7. Form a parallel beam

   - Brightness (LP):Form parallel beam by turning this know clock-wise (CW) until you obtain sharp diffraction spots
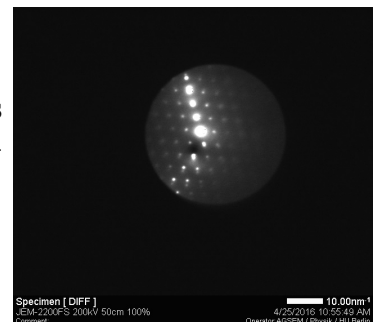

8. Remove high contrast aperture

   - Aperture control (LP): PUSH HCA + 0

9. Center non-diffracted beam

   - Projection lens alignment control / PLA (RP): center the non-diffracted beam

   - If non-diffracted beam can not be recognized than switch to image mode and move to thinner area of the specimen
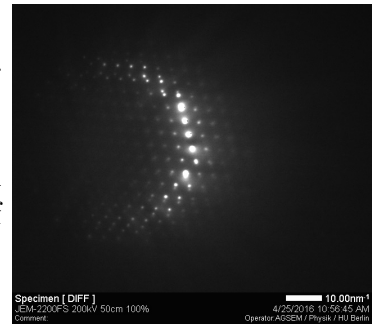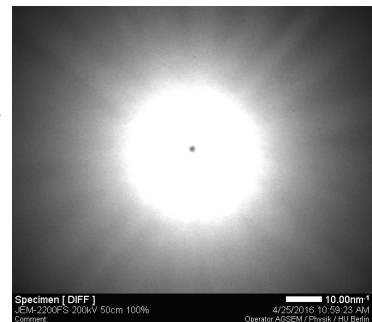

10. Visualize Kikuchi lines

    - Brightness (LP): condense the beam (turn CCW) to get convergent beam and to see the Kikuchi lines needed for zone axis alignment
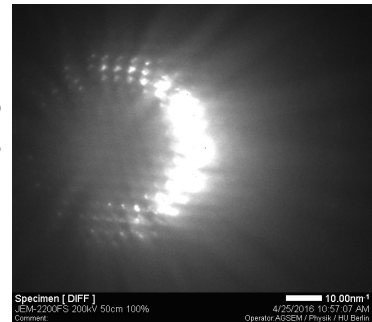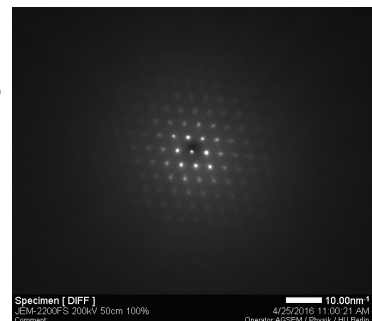

11. Orientate sample to zone axis

    - Tilt X and Y control (GP): adjust cross of Kikuchi lines ([110] zone axis) to center of diffraction pattern
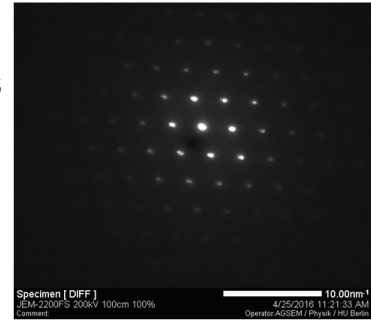

12. Form parallel beam

    - Brightness (LP): parallel beam by turning CW to form sharp diffraction spots
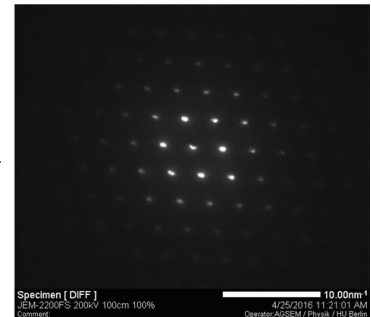
13. Enlarge camera length

   - MAG / CAM LENGTH (RP): Turn CW to adjust camera length to 100 cm

14. Center non-diffracted beam

   - Projector lens alignment / PLA (RP): Activate

   - DEF/STIG X and Y (LP and RP): Align non-diffracted beam to center of screen


15. Adjust interlens stigmator

   - Alignment panel for maintenance (software control PC monitor TEM): Activate IL STIG

   - DEF/STIG X and Y (LP and RP): Adjust to form circular spots

   - BRIGHTNESS (LP): Adjust to form sharp diffraction spots
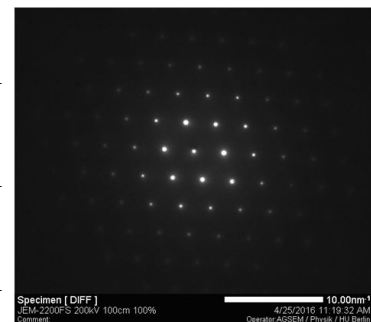
16. Measure distances of set of diffraction spots

   - Monitor screen (software control PC monitor TEM)

   - Acquire diffraction pattern by using the RECORD icon, store image

   - Measure distances from non-diffracted beam of the linearly independent spots

   - Calculate lattice plane distances and compare with tabulated values, index reflections, name crystal orientation, and define the calibration factor
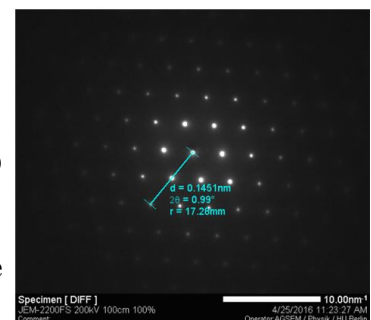
B. What you need to know about the JEOL JEM2200FS

Please refer to the document Instruction_ElectronDiffraction_2200FS.pdf

References

[1] H. Busch. Über die Wirkungsweise der Konzentrierungsspule bei der Braunschen Röhre. *Arch. Elektrotech. (Berlin)*, 18:583, 1927.

[2] J. M. Cowley and H. Shuman. Electron diffraction from a statistically rough surface. *Surface Science*, 38:53–59, 1973.

[3] A.V. Crewe, D.N. Eggenberger, J.Wall, and L.M.Welter. Electron gun using a field emission source. *Rev. Sci. Inst.*, 39:576, 1968.

[4] C. Davisson and L. H. Germer. Diffraction of electrons by a crystal of nickel. *Phys. Rev.*, 30:705–740, Dec 1927.

[5] C. Davisson and L. H. Germer. The scattering of electrons by a single crystal of nickel. *Nature*, 119:558–560, 1927.

[6] Louis de Broglie. *Recherches sur la theorie des quanta.* PhD thesis, Sorbonne, 1924.

[7] D. L. Dorset. *Structural Electron Crystallography.* Plenum, New York, 1995.

[8] P. A. Doyle and P. S. Turner. Relativistic Hartree-Fock X-ray and electron scattering factors. *Acta Cryst. A*, 24:390–397, 1968.

[9] H. W. Fink, H. Schmid, H. J. Kreuzer, and A. Wierzbicki. Atomic resolution in lensless low-energy electron holography. *Phys. Rev. Lett.*, 67:1543–1546, 1991.

[10] M. Haider, H. Rose, S. Uhlemann, E. Schwan, B. Kabius, and K. Urban. A spherical-aberration-corrected 200 kv transmission electron microscope. *Ultramicroscopy*, 75:53–60, 1998.

[11] C. Kisielowski, B. Freitag, M. Bischoff, H. van Lin, S. Lazar, G. Knippels, P. Tiemeijer, M. van der Stam an S. von Harrach, M. Stekelenburg, M. Haider, S. Uhlemann, H. Müller, P. Hartel, B. Kabius, D. Miller, I. Petrov, E.A. Olson, T. Donchev, E.A. Kenik, A.R. Lupini, J. Bentley, S. J. Pennycook, I. M. Anderson, A. M. Minor, A. K. Schmid, T. Duden, V. Radmilovic, Q.M. Ramasse, M. Watanabe, R. Erni, E.A. Stach, P. Denes, and U. Dahmen. Detection of single atoms and buried defects in three dimensions by aberration-corrected electron microscope with 0.5 a information limit. *Microsc. Microanal*, 14:469–477, 2008.

[12] M. Knoll and E. Ruska. Das elektronenmikroskop. *Z. Phys. A*, 78:318–339, 1932.

[13] O. L. Krivanek, N. Dellby, and A. R. Lupini. Towards sub-Å electron beams. *Ultramicroscopy*, 78:1–11, 1999.

[14] A. R. Moon and J. M. Cowley. Medium energy electron diffraction. *Journal of Vacuum Science and Technology*, 9:649–651, 1972.

[15] E. Ruska. The development of the electron microscope and of electron microscopy. *Reviews of Modern Physics*, 59:627–638, 1987.

[16] O. Scherzer. Über einige Fehler von Elektronenlinsen. *Z. Physik*, 101:593–603, 1936.

[17] J. C. H. Spence, U. Weierstall, and M. Howells. Phase recovery and lensless imaging by iterative methods in optical, X-ray and electron diffraction. *Phil. Trans. R. Soc. Lond. A*, 360:875–895, 2002.

[18] G. P. Thompson. Experiments on the diffraction of cathode rays. *Proceedings of the Royal Society of London. Series A, Containing Papers of a Mathematical and Physical Character*, 117:600–609, 1928.

[19] K. Vainshtein. *Structure Analysis by Electron Diffraction*. Pergamon, New York, 1964.

[20] T. E. Weirich, J. L. Lábár, , and X. Zou. *Electron Crystallography: Novel Approaches for Structure Determination of Nanosized Materials*, volume 211. Springer, Berlin, 2006.